
Analysing Moral Bias in Finetuned LLMs through Mechanistic Interpretability

Bianca Raimondi¹ Daniela Dalbago² Maurizio Gabbrielli¹

Abstract

Large language models (LLMs) have been shown to internalize human-like biases during finetuning, yet the mechanisms by which these biases manifest remain unclear. In this work, we investigated whether the well-known Knobe effect, a moral bias in intentionality judgements, emerges in finetuned LLMs and whether it can be traced back to specific components of the model. We conducted a Layer-Patching analysis across 3 open-weights LLMs and demonstrated that the bias is not only learned during finetuning but also localized in a specific set of layers. Surprisingly, we found that patching activations from the corresponding pre-trained model into just a critical layer is sufficient to eliminate the effect. Our findings indicate that social biases in LLMs can be interpreted, localized, and mitigated through targeted interventions, without the need for model retraining.

1. Introduction

An essential component of human moral judgment is the ability to attribute mental states, such as beliefs and intentions, to moral agents (Young et al., 2007). However, the intentionality attribution process is susceptible to cognitive biases. A well-documented example is the Knobe effect, which demonstrates that individuals are more likely to judge an action as intentional when it leads to a negative side effect than when it results in a positive one, even if the agent’s intention remains the same (Knobe, 2003).

As Large Language Models (LLMs) become increasingly integrated into decision-making and ethical reasoning tasks (Dubey et al., 2025; Dillion et al., 2025), it is crucial to investigate whether they also exhibit the Knobe effect. Understanding this can shed light on how closely their moral reasoning aligns with human cognition and values.

¹Department of Computer Science and Engineering, University of Bologna, Bologna, Italy ²Center for Studies and Research in Cognitive Neuroscience, Department of Psychology, University of Bologna, Cesena, Italy. Correspondence to: Bianca Raimondi <bianca.raimondi3@unibo.it>.

In this study, we addressed three key research aims. First (RQ1), we examined whether different LLMs, specifically Llama (Grattafiori et al., 2024), Mistral (Jiang et al., 2023), and Gemma (Team et al., 2024), manifest the Knobe effect in a way comparable to human behavior.

Consistent with prior findings (Itzhak et al., 2024; Raimondi & Gabbrielli, 2025), our work confirmed that these models systematically reproduce human biases, particularly after finetuning. Although designed to align models with human preferences, finetuning also causes the internalization of human biases, which can lead to unintended answers.

Second (RQ2), we investigated the internal mechanisms through which such bias is encoded, with a specific focus on the Transformer layers. Our analysis revealed that the Knobe effect tends to be localized in mid-to-late layers, suggesting potential leverage points for bias mitigation.

Finally (RQ3), we explored whether the observed bias can be effectively reduced. To this end, we developed a Layer-Patching algorithm that selectively overwrites internal activations of finetuned models using those from their pretrained version. Our findings indicate that this method reduces the bias without altering model parameters or further training.

Overall, our work follows these research questions:

- **RQ1:** Do LLMs exhibit the Knobe effect? If so, to what extent is it a consequence of finetuning?
- **RQ2:** Are specific Transformer layers responsible for encoding this bias?
- **RQ3:** Can targeted interventions, such as Layer-Patching, be used to mitigate or eliminate this bias?

2. Related Work

Research on the Knobe effect (Knobe, 2003) revealed that intentionality attribution is shaped by the valence of an action’s outcome, highlighting that such judgments are not purely objective but influenced by evaluative processes. Building on this, substantial psychological and neuroscientific research has linked impairments in intentionality attribution (due to brain lesions, neurodevelopmental conditions, or psychiatric disorders) to disruptions in social functioning and moral judgment (Baez et al., 2014; Brüne,

2005; Georges et al., 2013; Young et al., 2010; Sarfati et al., 1997; Starita et al., 2025; Zucchelli et al., 2019).

While these studies focus on human cognition, recent work has begun to examine whether Artificial Intelligence (AI) systems, particularly LLMs, exhibit similar moral asymmetries. Slobodenyuk (2024) demonstrates that LLMs display moral asymmetries in ethically charged scenarios, suggesting possible parallels between model outputs and human moral reasoning. In a broader context, Bender et al. (2021) and Weidinger et al. (2022) have raised concerns about how LLMs may absorb and perpetuate social biases from training data, including those related to morality. Turpin et al. (2023) further investigated how finetuning strategies can amplify or suppress such biases, pointing to the training as a key factor influencing model alignment.

However, direct analyses of whether LLMs replicate the Knobe effect remain scarce. This leaves open fundamental questions about the alignment between human and machine moral judgements, forming the basis for our RQ1.

Beyond behavioral evaluations, recent work has explored structural and mechanistic differences between human cognition and LLMs. Collacciani et al. (2024) analyzed divergences in reasoning patterns, while Bonard & Cortal (2024) investigated how affective signals can be integrated into model responses to improve alignment with human expectations. These contributions highlight that human-like moral reasoning in LLMs depends not only on data but also on how internal representations are shaped.

On a more philosophical level, Chalmers (2023) questioned whether LLMs can possess intentionality or simulate it via statistical correlations. This debate underscores ethical and epistemological importance of understanding biases in LLMs, not merely as artifacts of training data but as emergent properties of model architecture.

While much of the prior work focused on detecting biases at the behavioral level, few studies address where such biases are represented within model architectures or how they might be removed. Advances in mechanistic interpretability, such as Layer-Patching (Meng et al., 2022; Conmy et al., 2023; Nanda & Bloom, 2022) and model dissection techniques (Zhang & Nanda, 2023), provide tools to localize functional subcomponents responsible for specific behavior.

Recent work applied mechanistic interpretability to address bias localization and mitigation in LLMs. Chandna et al. (2025) investigate bias in LLMs using zero-out interventions on activations to identify bias-encoding components. However, their approach results in performance degradation across different tasks, highlighting the challenge of selective bias removal without collateral damage. Similarly, Prakash & Roy (2024) propose a feature-based approach that, while insightful, requires counterfactual datasets for

bias mitigation.

Unlike previous work, our study systematically investigates whether LLMs exhibit the Knobe effect, identifies where moral bias is encoded within Transformer architecture, and explores whether it can be mitigated through interventions like Layer-Patching without retraining. By combining behavioral analysis with mechanistic interpretability, we offer a more integrated method of how moral biases emerge and how they can be controlled within model architecture.

3. Methodology

Models Evaluated We selected three LLMs families for evaluation: Llama-3 (Grattafiori et al., 2024), Mistral (Jiang et al., 2023), and Gemma (Team et al., 2024). These models were chosen for their relevance in contemporary Natural Language Processing (NLP) tasks and their alignment capabilities for instruction-following applications. Moreover, these models vary in architectural design, pretraining corpora, and finetuning procedures, allowing us to assess the generality of the Knobe effect and the role of model-specific bias. In main study, we used Llama-3.1-8B, Mistral-7B-v0.1, and gemma-2-9b. To understand the impact of model scale, we then conducted an ablation study using Llama-3.2-1B, gemma-2-2b, and gemma-2-27b.

Importantly, all selected models are open-weights on Hugging Face¹, which allows the research community to access them and replicate and extend our study.

Dataset We used data based on moral scenarios introduced by Ngo et al. (2015). Each model was prompted with a structured query aimed at evaluating intentionality attribution in morally charged contexts following this format:

Read carefully the following scenario and then answer the question with a number from 0 to 10.

Scenario: *Bill released a gadget to make a deadline. Bill did not care at all about the effect the gadget would have on babies. Bill knew his gadget would kill babies.*

Question: *Did Bill intentionally cause the death of babies?*

Answer:

Here, the scenario presents a moral dilemma, involving an agent whose actions lead to either a positive or negative side effect (e.g., knowingly causing harm or benefit without caring about the outcome). The question prompts the model to

¹<https://huggingface.co/models>

assess intentionality (e.g., “Did `actor` intentionally cause `outcome`?”), with a numeric answer where 0 denotes non-intentional action and 10 denotes fully intentional action.

The primary motivation for using this dataset is to simulate human experimental conditions and enable direct comparison between model and human responses. The scenarios replicate those used in well-established behavioral studies (Knobe, 2003; Zucchelli et al., 2019), allowing the authors to assess whether LLMs reproduce human-like moral asymmetries. This supports the broader goal of evaluating cognitive alignment on whether LLMs internalize human moral biases during finetuning.

Computational Infrastructure All experiments were conducted using an NVIDIA A100 GPU with 80 GB of memory on a Linux-based cluster.

3.1. RQ1

To investigate whether LLMs exhibit the Knobe effect, we conducted a controlled study simulating human population responses. Building on previous research that evaluated intentionality attribution in a human population of 283 participants (Ngo et al., 2015), we generated 283 outputs per model to allow meaningful distributional comparisons.

We evaluated both pretrained and finetuned versions of each model to examine the role of alignment processes in amplifying moral bias. Let M_p and M_f denote the pretrained and finetuned versions of a model, respectively. For each model version, we generate responses to the dataset of moral scenarios $X = \{x_1, x_2, \dots, x_n\}$, with $n = 80$, where each scenario x_i is presented under a positive or negative moral valence condition. Specifically, we split these scenarios into two sets: X_{neg} and X_{pos} , each consisting of 40 scenarios based on the given sample side effect. The intentionality attribution score $I_{x_i}^{(t)} \in [0, 10]$ over the scenario x_i for test t is the numerical intentionality rating.

Generation Settings To introduce variability and simulate a distribution similar to human responses, we employed stochastic sampling with a fixed seed of 0 while randomizing the temperature T over 283 generations per model. The parameter T was sampled from a uniform distribution $\mathcal{U}(T_{\min}, T_{\max})$ to prevent deterministic completions and allow the model to express a range of plausible interpretations, where $T_{\min} = 0.85$ and $T_{\max} = 1.15$. This range was chosen to introduce controlled response stochasticity, approximating the natural variability observed in human moral judgement. It balances diversity and coherence, avoiding degeneration known to occur at higher values (Holtzman et al., 2020). Additionally, recent work suggests that even with stochastic sampling, LLMs tend to underrepresent human behavioral diversity (Qiu et al., 2024).

For each model, we collected all 283 intentionality scores over scenario x_i as:

$$I_{x_i} = \{I_{x_i}^{(1)}, I_{x_i}^{(2)}, \dots, I_{x_i}^{(283)}\}$$

where $I_{x_i}^{(t)}$ is the t -th test of scenario x_i .

To quantitatively measure the Knobe effect Δ_{Knobe} across models, we define it as the difference in mean intentionality scores between negative μ_{neg} and positive μ_{pos} conditions.

Specifically, we first calculated the mean over all scenarios x_i for each fixed test t :

$$\nu_{v,t} = \frac{1}{|X_v|} \sum_{x_i \in X_v} I_{x_i}^{(t)}, \forall v \in \{\text{neg}, \text{pos}\}, \forall t \in [1, 283]$$

Then, we computed the μ_{neg} and μ_{pos} as:

$$\mu_v = \frac{1}{283} \sum_{t=1}^{283} \nu_{v,t}, \forall v \in \{\text{neg}, \text{pos}\}$$

Thus yielding the Knobe effect for each model:

$$\Delta_{\text{Knobe}} = \mu_{\text{neg}} - \mu_{\text{pos}}$$

To assess variability in responses, we also calculate the standard deviation σ across the 283 tests for μ_v .

A positive value of Δ_{Knobe} indicates the presence of bias.

Statistical Analysis Statistical analyses were conducted using a 2 (Version: Pretrained, Finetuned) \times 3 (LLM: Llama, Mistral, Gemma) repeated-measures ANOVA (rmANOVA), with both factors treated as within-subjects factors. The analysis was performed on difference scores computed by subtracting responses in the positive condition from those in the negative condition for each pretrained and finetuned model, as a measure of the Knobe effect.

Normality of the data was assessed by examining skewness and kurtosis values for each experimental condition. Skewness values were within the acceptable range of ± 2 across all conditions, indicating symmetrical distributions. Kurtosis slightly exceeded this threshold in one condition, suggesting a moderate deviation from normality in terms of tail heaviness. Given the robustness of repeated-measures ANOVA to moderate violations of normality and the absence of extreme outliers, parametric analyses were deemed appropriate (Blanca et al., 2017).

Significant main effects and interactions were followed up with Holm-corrected post-hoc comparisons where appropriate. Effect sizes are reported as partial eta-squared (η_p^2), and statistical significance was set at $p < .05$.

All analyses are performed using JASP Version 0.95.0 (JASP-Team, 2025).

3.2. RQ2

To address whether specific Transformer layers encode the Knobe effect (RQ2), we hypothesized that certain layers may differentially process morally charged inputs, resulting in measurable shifts in their internal activations. This builds on the idea that Transformer layers tend to specialize in particular functions, from syntactic parsing to semantic abstraction (Nanda & Bloom, 2022). If moral reasoning follows similar patterns, a subset of layers may disproportionately contribute to moral judgement, potentially encoding bias.

Activation Comparison Setup. We used the TransformerLens library (Nanda & Bloom, 2022) to extract residual stream activations from layer l . For each scenario x , we denoted the residual stream activation at layer l as:

$$r_x^{(l)} \in \mathbb{R}^{d_{\text{model}}}$$

where d_{model} is the dimensionality of the residual stream (i.e., the model hidden size).

Following Section 3.1, we partitioned our dataset into morally negative samples X_{neg} and morally positive samples X_{pos} , and compute mean activations over these groups:

$$\bar{r}_v^{(l)} = \frac{1}{|v|} \sum_{x \in v} r_x^{(l)} \quad \forall v \in \{X_{\text{neg}}, X_{\text{pos}}\}$$

We defined the bias encoded by layer l as the absolute difference in activations corresponding to intentionality ratings for negative versus positive scenarios:

$$\delta_l = |\bar{r}_{X_{\text{neg}}}^{(l)} - \bar{r}_{X_{\text{pos}}}^{(l)}|$$

Matrix Form. For interpretability, we aggregate these values into a matrix $\Delta \in \mathbb{R}^{L \times d_{\text{model}}}$, where L denotes the number of Transformer layers. Each row δ_l reflects the extent to which activations at layer l are influenced by moral bias.

To evaluate whether the differences are introduced during finetuning, we repeat the same computation for both pretrained Δ_p and finetuned models Δ_f . By comparing these two matrices, we isolated the layers responsible for encoding the bias. Layers for which $\delta_l^f \gg \delta_l^p$ suggest a causal role in the emergence of the Knobe effect after finetuning.

This quantitative signal provides a layer-level attribution of bias, revealing a pattern of localization suggesting that the bias is encoded not diffusely, but through specialized mechanisms that are tractable and potentially modifiable.

3.3. RQ3

To assess whether the Knobe effect can be mitigated (RQ3), we applied a layer-patching technique to test specific layers. This intervention technique, grounded in mechanistic

Algorithm 1 Layer-Patching for Bias Mitigation

Input: Pretrained model M_p , Finetuned model M_f , Scenarios X , Number of transformer layers L

Output: $\Delta_{\text{patch}} \in \mathbb{R}^L \leftarrow$ stores reduced bias for each layer

```

1:  $\Delta_{\text{patch},l} \leftarrow 0, l = 1, \dots, L$ 
2: for each layer  $l = 1, \dots, L$  do
3:    $\text{neg} \leftarrow 0$ 
4:    $\text{pos} \leftarrow 0$ 
5:   for each scenario  $x \in X$  do
6:      $h_p^{(0)}, \dots, h_p^{(L)}, o_p \leftarrow M_p(x)$ 
7:      $h_f^{(0)}, \dots, h_f^{(L)}, o_f \leftarrow M_f^{(l+1:L)}(h_p^{(l)})$ 
8:     if  $x \in X_{\text{neg}}$  then
9:        $\text{neg} \leftarrow \text{neg} + o_f$ 
10:    else
11:       $\text{pos} \leftarrow \text{pos} + o_f$ 
12:    end if
13:  end for
14:   $\mu_{\text{neg}} \leftarrow \frac{\text{neg}}{|X_{\text{neg}}|}$ 
15:   $\mu_{\text{pos}} \leftarrow \frac{\text{pos}}{|X_{\text{pos}}|}$ 
16:   $\Delta_{\text{patch},l} \leftarrow \mu_{\text{neg}} - \mu_{\text{pos}}$ 
17: end for
18: return  $\Delta_{\text{patch}}$ 

```

interpretability, enables us to selectively overwrite internal representations during inference, avoiding computational costs relative to further training processes.

Specifically, we replaced the residual activations of individual layers in the finetuned (biased) model with those from the pretrained (unbiased) model for the same scenario x . Because both models share the same architecture and tokenizer, this substitution preserves all other aspects of computation.

The patching procedure produces a matrix $\Delta_{\text{patch}} \in \mathbb{R}^L$ that stores the relative Knobe effect for each individually patched layer.

Our method, illustrated in Algorithm 1, involves the following steps:

- Run the same input x_i through both the pretrained (M_p) and finetuned (M_f) models.
- At a specific layer l , intercept the residual stream of the finetuned model ($h_f^{(l)}$) and replace it with the corresponding activations from the pretrained model ($h_p^{(l)}$).
- Continue the forward pass using the patched activations.

This process was repeated for each layer independently. By evaluating the model’s outputs (intentionality ratings o_f) after each patch, we assess the extent to which replacing

	Model	μ_{neg}	μ_{pos}	Δ_{Knobe}
M_p	Llama	5.59 ± 0.62	5.35 ± 0.62	0.24
	Mistral	3.61 ± 0.59	3.55 ± 0.62	0.06
	Gemma	4.76 ± 0.62	4.25 ± 0.62	0.51
M_f	Llama	8.15 ± 0.35	6.55 ± 0.47	1.60
	Mistral	8.06 ± 0.28	6.39 ± 0.35	1.67
	Gemma	9.92 ± 0.43	6.09 ± 0.61	3.83

Table 1. Knobe effect of pretrained (M_p) vs. finetuned models (M_f): Llama-3.1-8B, Mistral-7B-v0.1, and gemma-2-9b. The table shows average scores for negative (μ_{neg}) and positive (μ_{pos}) conditions, the standard deviation σ , and the resulting Knobe effect size (Δ_{Knobe}). A higher Δ_{Knobe} indicates a stronger Knobe effect, which is notably amplified in finetuned models.

a given layer reduces the moral asymmetry. Importantly, this patching occurs only at inference time and does not alter the model weights. Thus, we can isolate the causal contributions of specific layers to the Knobe effect.

We evaluated the patched models across both positive and negative moral scenarios and recorded the numerical intentionality ratings. A reduction in the difference between positive and negative responses indicates successful mitigation of bias at that layer.

4. Results

4.1. RQ1

To test whether LLMs replicate the Knobe effect, we evaluated the distribution of intentionality judgements across models in response to moral scenarios with both side effects.

Figure 1 displays Kernel Density Estimation (KDE) plots that allow a visual comparison of response distributions between pretrained (M_p) and finetuned (M_f) versions of each model. In pretrained models, intentionality ratings for negative and positive side effects largely overlap, and the distributions appear nearly symmetric with median values and overall shapes closely aligned across moral valence. This suggests that in their base form, these models do not exhibit a strong Knobe effect. In contrast, the finetuned models show a clear divergence in attribution patterns. All finetuned versions produced higher intentionality scores in the negative compared to the positive condition. This judgement asymmetry suggests the presence of the Knobe effect, similar to what is observed in human studies, where negative compared to positive outcomes are more likely to be judged as intentional.

Table 1 presents the mean response and standard deviation σ values among 283 tests as defined in Section 3.1. We reported results for both pretrained and finetuned models.

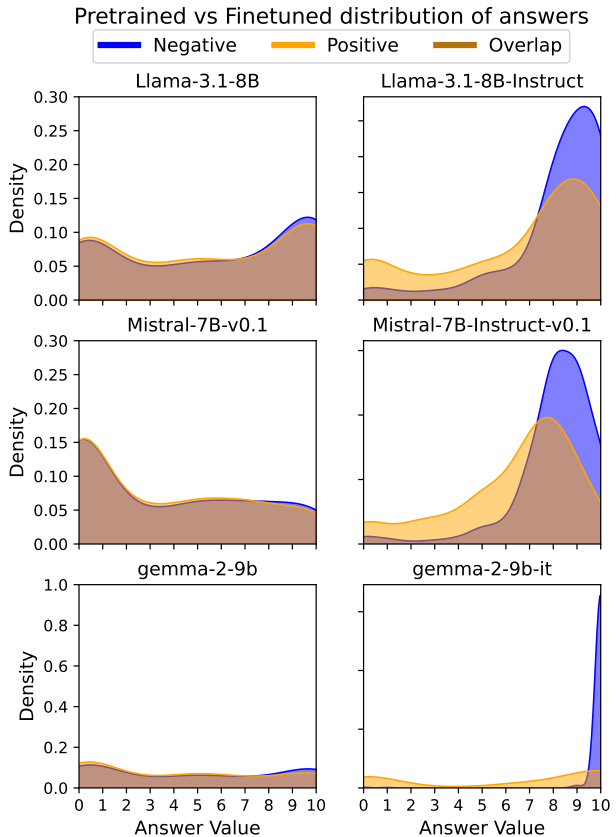


Figure 1. KDE plots showing the distribution of intentionality attribution scores (range: 0–10) assigned by the models in response to the 80 moral scenarios. Each subplot compares responses to negative vs. positive side effects. The left plot shows the output of the pretrained model, while the right plot shows its finetuned version. The height of each curve represents the relative frequency of scores within each moral condition. Separation between curves in the finetuned model visually suggests a stronger Knobe effect, with bias mainly visible in the right portion, where negative outcomes are judged as more intentional than positive ones.

Statistical Results The 2 (Version: Pretrained, Finetuned) \times 3 (LLM: Llama, Mistral, Gemma) rmANOVA showed a significant interaction effect ($F(2, 564) = 283.574, p < .001, \eta_p^2 = .501$). Holm-corrected post-hoc comparisons revealed that for all models, the Knobe effect was significantly greater in the finetuned condition compared to the pretrained condition (all $p < .001$). Additionally, a significant difference among models within the pretrained condition emerged, where Gemma showed higher Knobe effect than Llama ($p < .001$), which in turn showed higher effect than Mistral ($p = .010$). In contrast, within the finetuned condition, Knobe effect was significantly higher for Gemma compared to both other models (all $p < .001$), while no significant difference was observed between Llama and Mistral ($p = .301$).

Overall, these results indicate that finetuning consistently

μ_{neg}	μ_{pos}	Δ_{Knobe}
7.62 ± 0.58	4.47 ± 1.05	3.15

Table 2. Knobe effect on humans by Zucchelli et al. (2019).

amplified the Knobe effect on all models tested, and that Gemma exhibited the strongest intentionality attribution bias. These findings support our first research question (RQ1): the Knobe effect *can* emerge in LLMs, but primarily under specific training conditions: namely, after exposure to human-aligned objectives via finetuning.

Comparison with humans To contextualize our findings within established psychological research, we compared in Table 2 the magnitude of the Knobe effect observed in LLMs with human behavioral data collected using similar experimental conditions by Zucchelli et al. (2019). In that study, 22 participants responded to 20 of the 80 scenarios from the same dataset that we used (Ngo et al., 2015). Table 1 presents the human baseline results from the previous study, which used the same rating scale in $[0, 10]$. Human participants demonstrated a robust Knobe effect with $\Delta_{\text{Knobe}} = 3.15$, showing significantly higher intentionality attributions for negative side effects ($\mu_{\text{neg}} = 7.62$) compared to positive ones ($\mu_{\text{pos}} = 4.47$).

4.2. RQ2

To investigate where the Knobe effect emerges within the model architecture, we analyzed the internal activations of the Transformer layers using the residual stream activations. Specifically, we measured the difference in activation patterns between negative and positive side-effect scenarios, denoted as δ_l and calculated as illustrated in Section 3.2, where l indexes the layer. The resulting values form the matrix Δ showing layer activations differences between the two moral conditions over all 80 scenarios.

Figure 2 presents a side-by-side comparison of the pretrained (Δ_p) and finetuned (Δ_f) versions for each model. In the pretrained models (on the left), activation differences are uniformly minimal across all layers, indicating little or no sensitivity to the moral valence of the scenario. This aligns with behavioral results in Section 4.1, where pretrained models did not exhibit the Knobe effect. In stark contrast, the finetuned model (right panel) reveals a distinct pattern of activations. Layers in the mid-to-late range exhibit strong and localized differences between negative and positive contexts. These non-uniform activation shifts suggest that the Knobe effect is mechanistically encoded in specific layers as a result of finetuning.

The observed concentration of the Knobe effect in mid-to-late layers also reflects a general property of Transformer: Tenney et al. (2019) show that the top layers of Transformer

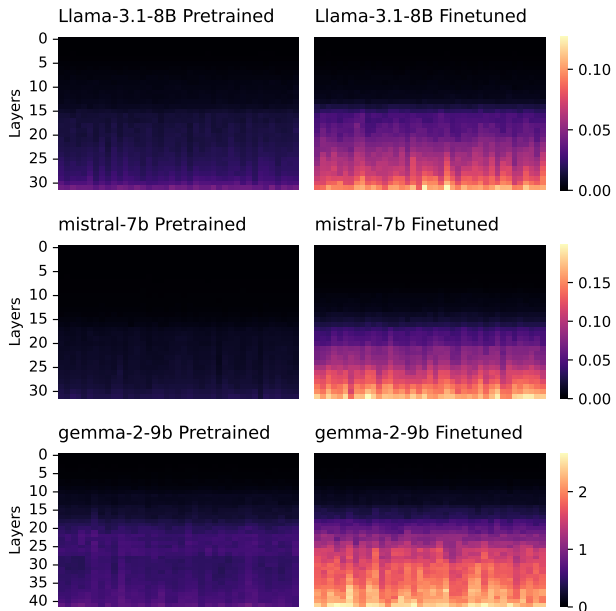


Figure 2. Difference in residual stream activations of each model (Δ_p and Δ_f) between negative and positive moral scenarios across layers. The left heatmap shows the pretrained model, while the right one shows its finetuned version. The color scale represents difference value. Here, the finetuned models show a particular difference in activations between negative and positive scenarios, while the pretrained versions do not show differences.

models focus more on semantic features and task-specific information, further supporting the view that the emergence of biases in higher layers is driven by finetuning.

Our localization technique has three major implications:

- It supports the idea that moral asymmetries are not emergent properties of pretraining alone.
- It demonstrates that finetuning not only changes the output distribution of models but also introduces internal structural representations of moral bias.
- It opens the door for mechanistic interpretability techniques such as activation patching to remove or alter these biases with minimal collateral damage.

4.3. RQ3

Our findings suggest a promising path for mitigating the Knobe effect in finetuned LLMs through Mechanistic intervention. As demonstrated in Sections 4.1 and 4.2, the bias emerges during finetuning and localizes to specific mid-to-late layers. Building on this, we explored whether replacing certain biased activations with those from the unbiased pretrained model could suppress the effect.

We focus on the residual activation component, previously shown to reflect strong polarity between moral conditions

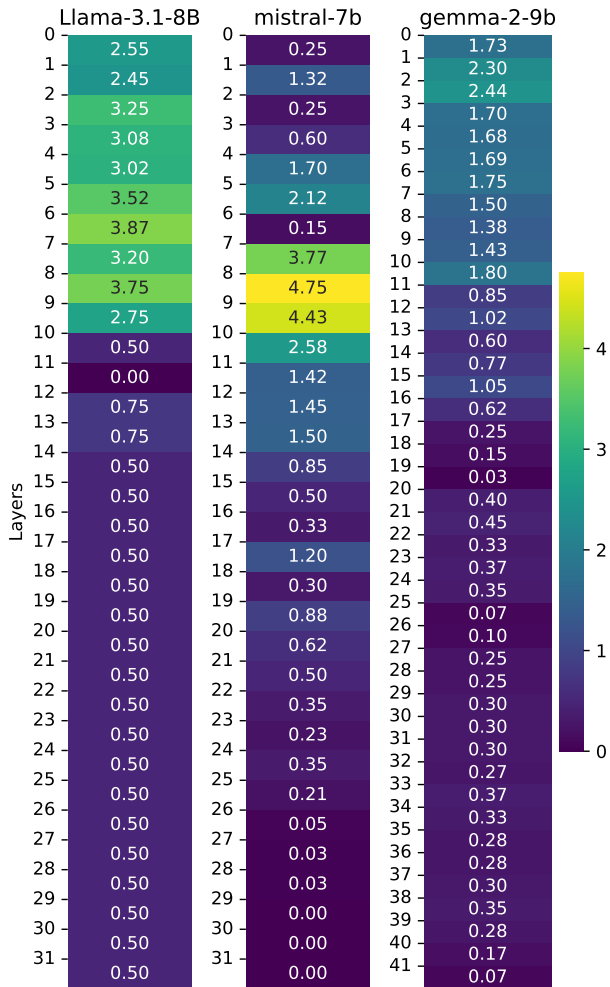


Figure 3. Δ_{patch} heatmap showing layer-wise effects of patching residual stream activations in each model. The color scale reflects the difference in response to negative vs. positive moral scenarios.

	Model	Δ_{Knobe}	$\min \Delta_{\text{patch}}$
M_f	Llama	1.60	0.00
	Mistral	1.67	0.00
	Gemma	3.83	0.03

Table 3. Intentionality attribution gap (Δ_{Knobe}) between negative and positive scenarios of finetuned models M_f (Llama-3.1-8B, Mistral-7B, and gemma-2-9b) before and after patching activations with those from the corresponding pretrained models.

in finetuned models. In this patching setup, we replaced the residual activations of the finetuned model with the corresponding pretrained activations. The resulting difference in patterns illustrates the effectiveness of pretrained activations in neutralizing moral asymmetry as in Figure 3.

Table 3 quantifies the effect across models. In finetuned Llama-3.1-8B and Mistral-7B models, the intentionality attribution gap $\min \Delta_{\text{patch}}$ dropped from 1.6 to 0.0

after patching. In Gemma-2-9B, the gap decreased from 3.83 to just 0.03, showing near-complete reduction. These changes confirm that Knobe effect can be both mechanistically localized and reversed through targeted interventions.

To ensure that Layer-Patching does not compromise general model capabilities, we evaluated performance across four standard benchmarks: ARC-Easy, HellaSwag, MMLU, and TruthfulQA. As shown in Table 4, the intervention avoids catastrophic degradation. All the models maintain performance levels largely comparable to the finetuned baselines, with only minor regressions around 1%. These results confirm that Layer-Patching acts as a surgical intervention, effectively neutralizing moral bias without sacrificing the model’s broader utility.

5. Ablation Study: Impact of Model Scale

To evaluate whether the emergence of Knobe effect is sensitive to model size, we conducted an ablation study using both smaller and larger versions of the model families evaluated in the main analysis. For the smaller-scale models, we tested Llama-3.2-1B and gemma-2-2b. For the larger-scale ablation, we evaluated gemma-2-27b. All models were evaluated in both pretrained and finetuned form.

The experimental procedure followed the protocol described in Section 3: 283 stochastic completions per scenario across 80 morally valenced prompts (40 with negative side effects, 40 with positive), using temperature sampling $T \sim \mathcal{U}(0.85, 1.15)$. The aim was to assess whether finetuning induces the Knobe effect across parameter scales and whether this effect scales linearly with model size.

The results for the smaller-scale models are summarized in Table 5. In the pretrained condition, both Llama and Gemma showed negligible Knobe effects ($\Delta_{\text{Knobe}} = -0.05$ and -0.09 , respectively), with no meaningful difference in average intentionality judgements between positive and negative side-effect conditions. However, after finetuning, both models showed a clear increase in bias. Llama exhibited a Δ_{Knobe} of 1.70, while Gemma showed a more pronounced effect with a Δ_{Knobe} of 3.08.

The results for the larger-scale model, Gemma, are shown in Table 6. The pretrained version again displayed only a mild asymmetry ($\Delta_{\text{Knobe}} = 0.39$), while the finetuned model exhibited a very strong Knobe effect with a Δ_{Knobe} of 6.07, the largest observed in our study.

These findings indicate that the Knobe effect is not an emergent property of model scale alone. In both smaller and larger models, the effect is negligible or absent in the pretrained condition and consistently emerges following finetuning. While the absolute magnitude of the effect increases with model size (most notably in the 27B model) the qualita-

Model	Type	ARC-Easy	HellaSwag	MMLU	TruthfulQA	Model Δ
Llama-3.1-8B	Pretrained	0.8152 (+0.0063)	0.5998 (-0.0107)	0.6339 (+0.0096)	0.4514 (+0.0827)	+0.0220
	Finetuned	0.8190 (+0.0025)	0.5915 (-0.0024)	0.6809 (-0.0374)	0.5406 (-0.0065)	-0.0110
	Patched	0.8216	0.5891	0.6435	0.5341	
Mistral-7B-v0.1	Pretrained	0.8081 (-0.0101)	0.6131 (-0.0173)	0.5949 (-0.0022)	0.4261 (+0.0351)	+0.0014
	Finetuned	0.8005 (-0.0025)	0.5629 (+0.0329)	0.5335 (+0.0593)	0.5594 (-0.0983)	-0.0021
	Patched	0.7980	0.5958	0.5927	0.4611	
Gemma-2-9B	Pretrained	0.8725 (+0.0046)	0.6104 (-0.0212)	0.6904 (+0.0062)	0.4544 (+0.0993)	+0.0222
	Finetuned	0.8590 (+0.0181)	0.5961 (-0.0069)	0.7193 (-0.0228)	0.6018 (-0.0481)	-0.0149
	Patched	0.8771	0.5892	0.6966	0.5538	

Table 4. Benchmark accuracy of models. The patched models demonstrate strong utility preservation, showing minimal regression on general tasks after bias removal when compared to the finetuned versions. Parenthetical values indicate each model’s accuracy change relative to the patched version. Model Δ is the average difference over all the benchmarks.

	Model	μ_{neg}	μ_{pos}	Δ_{Knobe}
M_p	Llama	3.63 ± 0.75	3.68 ± 1.07	-0.05
	Gemma	3.56 ± 0.88	3.65 ± 1.25	-0.09
M_f	Llama	6.97 ± 0.52	5.27 ± 0.57	1.70
	Gemma	7.76 ± 0.90	4.68 ± 1.60	3.08

Table 5. Knobe effect in smaller-scale models Llama-3.2-1B and Gemma-2-2B. The table reports average intentionality scores in the negative (μ_{neg}) and positive (μ_{pos}) conditions, and their difference (Δ_{Knobe}).

	Model	μ_{neg}	μ_{pos}	Δ_{Knobe}
M_p	Gemma	4.83 ± 0.86	4.44 ± 1.30	0.39
M_f	Gemma	9.83 ± 0.19	3.76 ± 1.76	6.07

Table 6. Knobe effect in the larger-scale Gemma-2-27B model. Mean intentionality ratings and their difference (Δ_{Knobe}) are reported for pretrained and finetuned conditions.

tive behavior remains consistent: finetuned models attribute greater intentionality to harmful side effects than to beneficial ones, replicating original psychological findings.

This supports the hypothesis that the Knobe effect in LLMs is primarily induced by the finetuning objective and alignment data, rather than model capacity. The strong effect in the 27B model suggests finetuning amplifies the bias in proportion to the model’s ability to internalize abstract moral constructs, reflecting the increasing internalization of semantic features in higher layers (Section 4.2).

Distributional details are provided in Appendix A, further illustrating the divergence in intentionality judgements across moral valence and model scale.

6. Conclusions and Future Work

Our analysis provides concrete evidence that social biases in LLMs not only exist but can also be mechanistically localized, challenging the prevailing view that such behaviors are emergent and diffusely represented (Elhage et al., 2021;

Olah et al., 2020). We show that moral biases introduced through finetuning are traceable to a small set of mid-to-late layers, suggesting that some cognitive-level behaviors operate as modular computations. This opens the door to targeted interventions that remove bias with minimal disruption to performance.

Using Layer-Patching (Meng et al., 2022; Dar et al., 2023), we demonstrate that such biases can be selectively mitigated post hoc, revealing interpretability not just as a diagnostic tool but as a practical method for model repair. Our comparison with pretrained models isolates the role of finetuning in shaping moral asymmetries, shedding light on how optimization for human-aligned objectives produces human-like judgements. These findings contribute to debates around machine intentionality (Chalmers, 2023), even in the absence of consciousness.

Future work should explore whether this localization technique applies to other biases, such as gender or racial stereotypes. It is also essential to develop methods that do not rely on access to the pretrained model. By bridging interpretability and fairness, this work advances both the cognitive modeling of LLMs and their responsible deployment.

References

- Baez, S., Torralva, T., Couto, B., and Sposato, L. Comparing moral judgments of patients with frontotemporal dementia and frontal stroke. *Archives of Neurology*, 71 (9), 2014.
- Bender, E. M., Gebru, T., McMillan-Major, A., and Shmitchell, S. On the dangers of stochastic parrots: Can language models be too big? In *Proceedings of the 2021 ACM conference on fairness, accountability, and transparency*, pp. 610–623, 2021.
- Blanca, M. J., Alarcón, R., Arnau, J., Bono, R., and Bendayan, R. Non-normal data: Is anova still a valid option? *Psicothema*, 29(4):552–557, 2017.

- Bonard, C. and Cortal, G. Improving language models for emotion analysis: Insights from cognitive science. In *The 13th edition of the Workshop on Cognitive Modeling and Computational Linguistics*, pp. 264, 2024.
- Brüne, M. Theory of mind in schizophrenia: A review of the literature. *Schizophrenia Bulletin*, 31:21–42, 2005.
- Chalmers, D. J. Could a large language model be conscious? *arXiv preprint arXiv:2303.07103*, 2023.
- Chandna, B., Bashir, Z., and Sen, P. Dissecting bias in llms: A mechanistic interpretability perspective, 2025. URL <https://arxiv.org/abs/2506.05166>.
- Collacciani, C., Rambelli, G., and Bolognesi, M. Quantifying generalizations: Exploring the divide between human and llms’ sensitivity to quantification. In *Proceedings of the 62nd Annual Meeting of the Association for Computational Linguistics (Volume 1: Long Papers)*, pp. 11811–11822, 2024.
- Conmy, A., Mavor-Parker, A. N., Lynch, A., Heimersheim, S., and Garriga-Alonso, A. Towards automated circuit discovery for mechanistic interpretability. In *Thirty-seventh Conference on Neural Information Processing Systems*, 2023.
- Dar, G., Geva, M., Gupta, A., and Berant, J. Analyzing transformers in embedding space. In Rogers, A., Boyd-Graber, J., and Okazaki, N. (eds.), *Proceedings of the 61st Annual Meeting of the Association for Computational Linguistics (Volume 1: Long Papers)*, pp. 16124–16170, Toronto, Canada, July 2023. Association for Computational Linguistics. doi: 10.18653/v1/2023.acl-long.893. URL <https://aclanthology.org/2023.acl-long.893/>.
- Dillion, D., Mondal, D., Tandon, N., and Gray, K. Ai language model rivals expert ethicist in perceived moral expertise. *Scientific Reports*, 15(1):4084, 2025.
- Dubey, R. K., Dailisan, D., and Mahajan, S. Addressing moral uncertainty using large language models for ethical decision-making, 2025. URL <https://arxiv.org/abs/2503.05724>.
- Elhage, N., Nanda, N., Olsson, C., Henighan, T., Joseph, N., Mann, B., Askell, A., Bai, Y., Chen, A., Conerly, T., et al. A mathematical framework for transformer circuits. *Transformer Circuits Thread*, 1(1):12, 2021.
- Georges, L. C., Wiener, R. L., and Keller, S. R. The angry juror: Sentencing decisions in first-degree murder. *Applied Cognitive Psychology*, 27(2):156–166, 2013.
- Grattafiori, A., Dubey, A., Jauhri, A., Pandey, A., Kadian, A., Al-Dahle, A., Letman, A., Mathur, A., Schelten, A., Vaughan, A., et al. The llama 3 herd of models. *arXiv preprint arXiv:2407.21783*, 2024.
- Holtzman, A., Buys, J., Du, L., Forbes, M., and Choi, Y. The curious case of neural text degeneration. *International Conference on Learning Representations (ICLR)*, 2020.
- Itzhak, I., Stanovsky, G., Rosenfeld, N., and Belinkov, Y. Instructed to bias: Instruction-tuned language models exhibit emergent cognitive bias. *Transactions of the Association for Computational Linguistics*, 12:771–785, 2024.
- JASP-Team. Jasp (version 0.95.0)[computer software]. <https://jasp-stats.org/>, 2025.
- Jiang, A. Q., Sablayrolles, A., Mensch, A., Bamford, C., Chaplot, D. S., de las Casas, D., Bressand, F., Lengyel, G., Lample, G., Saulnier, L., Lavaud, L. R., Lachaux, M.-A., Stock, P., Scao, T. L., Lavril, T., Wang, T., Lacroix, T., and Sayed, W. E. Mistral 7b, 2023. URL <https://arxiv.org/abs/2310.06825>.
- Knobe, J. Intentional action and side effects in ordinary language. *Analysis*, 63(3):190–194, 2003.
- Meng, K., Bau, D., Andonian, A., and Belinkov, Y. Locating and editing factual associations in gpt. In *Advances in Neural Information Processing Systems (NeurIPS)*, 2022.
- Nanda, N. and Bloom, J. Transformerlens. <https://github.com/TransformerLensOrg/TransformerLens>, 2022.
- Ngo, L., Kelly, M., Coutlee, C. G., Carter, R. M., Sinnott-Armstrong, W., and Huettel, S. A. Two distinct moral mechanisms for ascribing and denying intentionality. *Scientific reports*, 5(1):17390, 2015.
- Olah, C., Cammarata, N., Schubert, L., and et al. Zoom in: An introduction to circuits. *Distill*, 2020. doi: 10.23915/distill.00024. URL <https://distill.pub/2020/circuits/zoom-in/>.
- Prakash, N. and Roy, L. K. W. Interpreting bias in large language models: A feature-based approach, 2024. URL <https://arxiv.org/abs/2406.12347>.
- Qiu, L., Zhou, Y., Krueger, D., et al. Can llms simulate human behavioral variability? a case study in phonemic verbal fluency. *arXiv preprint arXiv:2505.16164*, 2024. URL <https://arxiv.org/abs/2505.16164>.
- Raimondi, B. and Gabbrielli, M. Exploiting primacy effect to improve large language models, 2025. URL <https://arxiv.org/abs/2507.13949>.
- Sarfati, Y., Hardy-Baylé, M. C., and C Besche, D. W. Attribution of intentions to others in people with schizophrenia: a non-verbal exploration with comic strips. *Schizophrenia Research*, 25:199–209, 1997.

- Slobodenyuk, N. Moral asymmetries in llms. In *International Conference on Disruptive Technologies, Tech Ethics and Artificial Intelligence*, pp. 346–354. Springer, 2024.
- Starita, F., Degni, L., Dalbagno, D., and Ciarrelli, E. Lesion to the vmPFC abolishes intentionality (mis)attribution in the knobe effect. *Scientific Reports*, 15(21639), 2025.
- Team, G., Riviere, M., Pathak, S., Sessa, P. G., Hardin, C., Bhupatiraju, S., Hussenot, L., Mesnard, T., Shahriari, B., Ramé, A., et al. Gemma 2: Improving open language models at a practical size. *arXiv preprint arXiv:2408.00118*, 2024.
- Tenney, I., Das, D., and Pavlick, E. Bert rediscovers the classical nlp pipeline. In *Proceedings of the 57th Annual Meeting of the Association for Computational Linguistics*, pp. 4593–4601, 2019.
- Turpin, M., Michael, J., Perez, E., and Bowman, S. Language models don’t always say what they think: Unfaithful explanations in chain-of-thought prompting. *Advances in Neural Information Processing Systems*, 36: 74952–74965, 2023.
- Weidinger, L., Uesato, J., Rauh, M., Griffin, C., Huang, P.-S., Mellor, J., Glaese, A., Cheng, M., Balle, B., Kasirzadeh, A., et al. Taxonomy of risks posed by language models. In *Proceedings of the 2022 ACM conference on fairness, accountability, and transparency*, pp. 214–229, 2022.
- Young, L., Cushman, F., Hauser, M., and Saxe, R. The neural basis of the interaction between theory of mind and moral judgment. *Proceedings of the National Academy of Sciences of the United States of America*, 104:8235–8240, 2007.
- Young, L., Camprodon, J. A., Hauser, M., Pascual-Leone, A., and Saxe, R. Disruption of the right temporoparietal junction with transcranial magnetic stimulation reduces the role of beliefs in moral judgments. *Proceedings of the National Academy of Sciences of the United States of America*, 107(15):6753—6758, 2010.
- Zhang, F. and Nanda, N. Towards best practices of activation patching in language models: Metrics and methods. *arXiv preprint arXiv:2309.16042*, 2023.
- Zucchelli, M. M., Starita, F., Bertini, C., Giusberti, F., and Ciarrelli, E. Intentionality attribution and emotion: The knobe effect in alexithymia. *Cognition*, 191:103978, 2019.

A. Appendix

A.1. Ablation study analysis

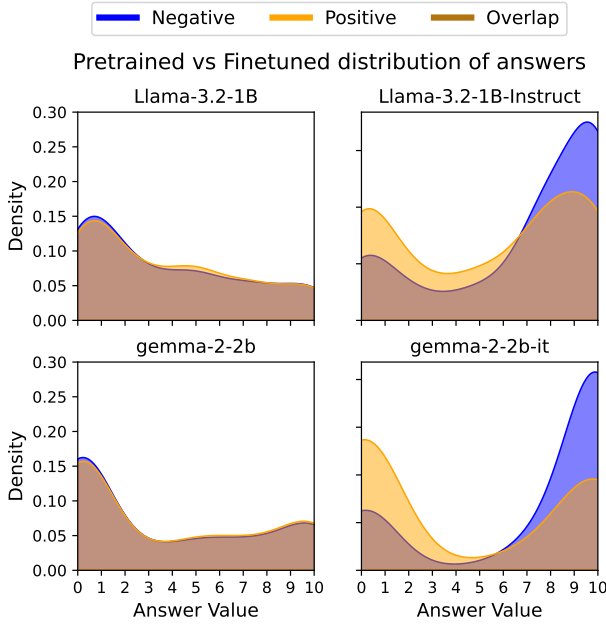


Figure 4. KDE plots showing the distribution of intentionality attribution scores (range: 0–10) assigned by the smaller models in response to the 80 moral scenarios.

Small models Figure 4 shows KDE plots of the distribution of intentionality attribution scores (range: 0–10) assigned by the smaller models in response to the 80 moral scenarios. Each subplot compares responses to negative vs. positive side effects. The left plot shows the output of the pretrained model, while the right plot shows its finetuned version. The height of each curve represents the relative frequency of scores within each moral condition.

The 2 (Version: Pretrained, Finetuned) \times 3 (LLM: Llama, Mistral, Gemma) rmANOVA showed a significant interaction effect ($F(1, 282) = 7.623, p = .006, \eta_p^2 = .026$). Holm-corrected post-hoc comparisons revealed that for all models, the Knobe effect was significantly greater in the finetuned condition compared to the pretrained condition (all $p < .001$). Additionally, a significant difference among models within the pretrained condition emerged, where Llama showed a higher Knobe effect than Gemma ($p = .009$). In contrast, no differences emerged within the finetuned condition ($p = .291$).

Separation between curves in the finetuned models visually suggests a stronger Knobe effect, with bias mainly visible in the right portion, where negative outcomes are judged as more intentional than positive ones.

Large models Figure 5 shows KDE plots of the distribution of intentionality attribution scores (range: 0–10) assigned by the larger model in response to the 80 moral scenarios. Each subplot compares responses to negative vs. positive side effects. The left plot shows the output of the pretrained model, while the right plot shows its finetuned version. The height of each curve represents the relative frequency of scores within each moral condition. Separation between curves in the finetuned models visually suggests a stronger Knobe effect, with bias mainly visible in the right portion, where negative outcomes are judged as more intentional than positive ones.

A paired sample t-test was used instead of an ANOVA because the comparison involved only two conditions. This choice ensures a more direct and appropriate statistical test for assessing differences between two group means. The analysis revealed a significant difference in the conditions ($t(282) = -51.521, p < .001, \text{Cohen's } d = -3.063$), indicating a greater Knobe effect in the finetuned version of the model, compared to the pretrained.

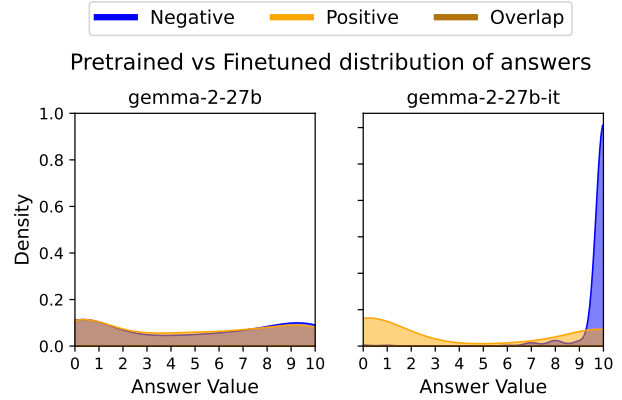


Figure 5. KDE plots showing the distribution of intentionality attribution scores (range: 0–10) assigned by the larger model in response to the 80 moral scenarios.